

See discussions, stats, and author profiles for this publication at: <https://www.researchgate.net/publication/344280406>

SYNTHESIS AND AB INITIO STUDY OF CRYSTAL CHEMISTRY OF A NOVEL MIXED VALENCE CUBICAL STRUCTURE OF $\text{Na}_{24}\text{Bi}_4\text{Cs}_8\text{Cl}_{26}$ VIA POWDER XRD METHOD

Article · September 2020

CITATIONS

0

READS

56

2 authors:



Rohit Kumar Dev

Bioinorganic and Materials Chemistry Research Laboratory, Mahendra Morang Adars...

7 PUBLICATIONS 0 CITATIONS

SEE PROFILE



Parashuram Mishra

Tribhuvan University

220 PUBLICATIONS 2,213 CITATIONS

SEE PROFILE

Some of the authors of this publication are also working on these related projects:



Lab work collaboration [View project](#)



Oxidation of Penicillanic acid derivatives / Techniques of degradation of antibiotics [View project](#)

SYNTHESIS AND *AB INITIO* STUDY OF CRYSTAL CHEMISTRY OF A NOVEL MIXED VALENCE CUBICAL STRUCTURE OF $\text{Na}_{24}\text{Bi}_4\text{Cs}_8\text{Cl}_{26}$ VIA POWDER XRD METHOD

Rohit K.Dev and Parashuram Mishra*, Bioinorganic and Materials Chemistry Research
Lab.M.M.A.M.Campus,Biratnagar,Tribhuvan University,Nepal

E-mail:chemistryprm@gmail.com

ABSTRACT

Sodium bismuth cesium chloride salt $\text{Na}_{24}\text{Bi}_4\text{Cs}_8\text{Cl}_{26}$ has been synthesized as polycrystalline powder by solid state reaction with followed stoichiometric chemistry. The structure has been determined by X-ray diffraction powder pattern ab initio method at room temperature. The title material is mixing in agate mortar and pastel in homogised form and was taking poder diffraction data in the cubical crystal system having space group $Fm\bar{3}m$ (225) with the unit cell parameters: $a=b=c$ 10.839 Å $V=273.41\text{Å}^3$ and $Z=2$. The two tools of crystal structure validation, Bond Valence Sum (BVS) and Charge distribution (CHARDI) methods, have confirmed the crystal structure model. The anionic framework is built of layers of corner sharing NaBi/Cl and CsCl_3 polyhedral structure. The sodium atoms are located in the interlayer space. Quantitative analysis using ICP-MS is used to confirm the elemental composition of the polycrystalline powder.. The electrical properties of the title compound have been characterized by impedance spectroscopy in the 240°C-360°C temperature range. At 240 °C, the conductivity value of the sample with relative density of 85% is $4 \cdot 10^{-6} \text{Scm}^{-1}$ and the activation energy was $E_a=0.76 \text{eV}$. The calculated conductivity corrected for porosity is $\sigma_d(240^\circ\text{C}) = 1.78 \cdot 10^{-5} \text{Scm}^{-1}$. The Na^+ transport pathway in the interlayer space was simulated using the Band Valence Site Energy (BVSE) model. The BVSE model was also used to explain the effect of the Cl/Cs on the electrical properties of the title compound.

KEYWORDS: Structure, Inter-layer Electrical properties, Transport pathways SEM,TEM,AFM

INTRODUCTION

Over the past decade, structure determination and study the crystal chemistry from powder XRD diffraction has matured into a technique that is widely and successfully used in the context of organic, inorganic, and organometallic compounds [1]. By definition, the crystal belonging to the same structure type with same space group should have the similar cell parameters and similar representative atom coordinates. But in the case of deficit materials like ternary compounds ($\text{Na}_{24}\text{Bi}_4\text{Cs}_8\text{Cl}_{26}$ compounds) which have different atomic defects, have

some major variations in the crystallographic parameters. Hence, the study of crystal structure of these compounds is necessary to understand its physical properties, especially the electronic properties. [1], which is important for many practical applications. For example, LiFePO₄ phosphate has successfully replaced LiCoO₂ oxide in lithium batteries [2]. Recently, research groups have concentrated on Na-ion batteries, as sodium is less toxic and is abundant in nature [3]. Numerous new compositions have been recently prepared and tested for electrical and/or electrochemical properties, e.g. NaCo(PO₃)₃ [4], Na₄Ni₃(PO₄)₂P₂O₇ [8], Na₂Ni₂Cr(PO₄)₃ [5], Na_{1.86}Fe₃(PO₄)₃ [6]. Sodium bismuth cesium chloride Na₂₄Bi₄Cs₈Cl₂₆ is a well-known material due to its low activation energy (0.63 eV) of ionic conductivity [7] and due to its higher thermal stability compared to the other chloride materials. The sodium atoms are located in the interlayer space, which is formed by sodium and bismuth polyhedra. This material is a good candidate as a cathode in Na-ion batteries given its crystal structure, thermal stability and presence of cesium metal. It has been shown recently to have reversible capacity close to 90 mA h g⁻¹ involving Bi⁺³/Bi⁺⁵ redox activity with an average potential of 3V [8]. The structure solution from powder X-ray diffraction and Rietveld refinement of some Na₂₄Bi₄Cs₈Cl₂₆. But the structural studies of Na₂₄Bi₄Cs₈Cl₂₆ lack a step in the literature. Materials with pronounced twinning or new compounds that only exist as part of a complex multi-phase powder sample are thus extremely difficult to treat with this standard method for structure determination [9]. It should be noted that these problem cases also include many technologically relevant products such as small precipitates in a metallic matrix, catalysts, pharmaceuticals, pigments and thin films, which a priori exist only in small quantities or rarely grow as large crystals. Hence, ample motivation exists to develop alternative approaches capable for structural analysis of extremely small volumes and crystallites. However, the only real alternative to X-rays is fast electrons, since their interaction with matter is several orders of magnitude stronger than that of X-rays. Electron diffraction structure analysis (EDSA) makes it, thus, possible to obtain structural information at the atomic level even for the steadily growing number of nanocrystalline materials [10]. On the other hand, structure analysis with electron data is rarely straightforward and fully automated, as it is the case with X-ray data. because now-a-days powder X-ray diffraction has been routinely used a non-destructive fingerprinting technique. It has also been used in studies related to structural phase transitions at variable temperature and pressure. Hence, the present study aims at the preparation of Na₂₄Bi₄Cs₈Cl₂₆ through the solid state reaction method and the determination of the structure of Na₂₄Bi₄Cs₈Cl₂₆ powders through powder X-ray diffraction technique. The extensive search for novel inorganic materials with open frameworks formed of tetrahedra and octahedra delimiting inter-layer spaces (2D), tunnels (3D) or cages (1D) where cations are housed, represent currently a field of intense activity including several disciplines: solid-state chemistry, physics, mechanics, and mainly ionic conductivity properties and their use as battery materials. Chloride of nontransition metals and alkaline cations are well known for their thermal stability and the simplicity of syntheses. The aim of this work is determine structure of titled compound by ab initio method with the help of powder XRD and the study of morphology as well as electrical property.

MATERIALS AND METHODS

All chemicals used were analytical grade. A polycrystalline sample of Na₂₄Bi₄Cs₈Cl₂₆ was synthesized by a standard solid state reaction using a mixture of high purity reagents of NaCl, BiCl₃ and CsCl contained mixed valence as the starting materials in the molar ratio of 3 :

1 : 1. The mixture was ground carefully, homogenized thoroughly with methanol (99%) in an agate mortar and then packed into an alumina crucible and calcined at 1000°C in air for 30h with several intermediate grindings. Finally the product was pressed into pellets and sintered at 100 K/h. Powder X-ray diffraction (XRD) data were collected at room temperature in the angular range of $2\theta = 10$ to 90 with scan step width of 0.02° and a fixed containing time of 15 s using Philips powder diffractometer with graphite monochromatic CuK α radiation. The powder was rotated during the data collection to minimize preferred Orientation effect if any. The program TREOR in CRYSFIRE was used to index the powder pattern which give cubic crystal system .SIRPOW92 was used to locate the positional parameters of constituent atoms. The full pattern is fitting and peak decomposition in the space group F m -3 m using check cell program. The structural parameters were refined by the Reitveld method using the JANA program which gave at 1000°C. Rwp = 0.0680, Rp = 0.030 and GOF=0.31 the structure factors F0 =3024 and Fc = 3024. The density is determined by Archimedes principle.

RESULTS AND DISCUSSION

In crystal chemistry, the crystal structure determination is the first step to understand and interpret physical properties of an unknown material. Moreover, it also guides people on how to modify the material and hence improve the performance[11].The extensive search for novel inorganic materials with open frameworks formed of tetrahedral and octahedral delimiting inter-layer spaces (2D), tunnels (3D) or cages (1D) where cations are housed, represent currently a field of intense activity including several disciplines: solid-state chemistry, physics, mechanics, and mainly ionic conductivity properties and their use as battery materials oxides of metals and alkaline cations are well known for their thermal stability and the simplicity of syntheses , which is important for many practical applications. lithium batteries [12]. Recently, research groups have concentrated on Na-ion batteries, as sodium is less toxic and is abundant in nature [8]. This material is a good candidate as a cathode in Bi⁺³ion batteries given its crystal structure, thermal stability and presence of Cs metal. It has been shown recently to have reversible capacity close to 80 mA h g⁻¹ involving Bi/Na redox activity with an average potential of 3V [13]. Nowadays, the most successful technique for structure determination is through single crystal X-ray diffraction, from which a sufficient number of independent reflections against the structural parameters can be extracted in 3D reciprocal space. Several mature analysis methods, such as the direct method,1 Patterson method,2 charge-flipping algorithm3 and maximum entropy method4 can be applied to accurately solve the structure. This technique requires synthesizing a high quality single crystal at a micrometer. Experimentally, the chance to get polycrystalline materials is generally larger than to get single crystals. In this case, powder X-ray diffraction (PXRD) becomes a popular technique but with this technique, the possibility to determine an unknown structure dramatically decreases, because 3D reflections are compressed into 1D with an inevitable overlapping problem, especially when the unit cell is big. The situation will become worse when the PXRD is collected on a multi-phase sample, which is not uncommon in the preliminary stage of searching new materials, especially in the cases of hydrothermal (or solvothermal) syntheses of zeolitic or MOF materials'XRD data for the sample of Na₂₄Bi₄Cs₈ Cl₂₆synthesized at its nominal composition is shown in Figure 1. All peaks could be indexed to acubic unit cell with F m -3 m (225) analogous to the Na₂₄Bi₄Cs₈ Cl₂₆ structure using CRYSFIRE PACKAGE[10]. In the diffraction pattern there is a slight anisotropic peak

broadening moving to higher angles. This slight peak broadening could be caused by ordering within the cationic layers but relative disorder of the cations between layers. The sloping background observed in XRD at low angles out to $\sim 30^\circ 2\theta$ is qualitatively indicative of stacking faults, a common feature of honeycomb chloride. In an ideal layered mixed-metal chloride contained mixed valence, all the cationic planes are stacked along the a-axis by a unique translational stacking vector. However it has been shown that two other stacking vectors with very similar energy (1-2 meV) can occur in a structure, leading to so called "stacking faults". Stacking faults in the honeycomb oxides occur due to the relatively weak coupling between the layers. In practice, the cationic layers are never perfectly stacked along the c-axis when a layered structure has the *P-1* space group, although higher temperature thermal treatment during synthesis can decrease the frequency of stacking faults [14].

CRYSTAL CHEMISTRY SOLUTIONS

High-resolution data set was collected for $\text{Na}_{24}\text{Bi}_4\text{Cs}_8\text{Cl}_{26}$ on a Philips powder diffractometer utilizing $\text{CuK}\alpha$ radiation. The powder XRD spectra shown in figure 1. The Rietveld refinement was done using the JANA2006 software. As in the case of $\text{Na}_{24}\text{Bi}_4\text{Cs}_8\text{Cl}_{26}$ [15], indexing the powder patterns was not straightforward as two sets of Miller indices are possible for the strongest reflections yielding two alternative unit cells which led to close residuals upon Le Bail full-pattern decomposition. Subsequent Rietveld refinements clearly ruled out one of these due to intolerably dissimilar Bi-Cl distances in the chloride anion. Final Rietveld refinement plot $\text{Na}_{24}\text{Bi}_4\text{Cs}_8\text{Cl}_{26}$ is given in Figure. 3; general projection of the cubical crystal structure is shown in Figure 2; the refinement results are collected in Tables 1. For $\text{Na}_{24}\text{Bi}_4\text{Cs}_8\text{Cl}_{26}$ structures was refined from routine XRD data to confirm the same atomic arrangement; these refinements also converged to reasonable R values. Just traces of by-products were present which could not be identified as their estimated content is below 1%. The Na ion coordinated with Cl atom having octahedral geometry and Cs atom ion also coordinated as same while Bi ions coordinated triangular bipyramidal structure. Structure of cited compound is face-centre-cubic (FCC). The first step of the structure determination consisted to localize the positions of heavy atoms (cations). The Monte Carlo analysis in the Diamond software program [16] was launched in scratch mode using only the first 230 peaks (extracted by Le Bail refinement from the XRD data in space group $Fm\bar{3}m$). The crystallographic data obtained from Rietveld refinement which shown in table 1. For the determination of cationic positions, in order to minimize the number of different atom types, we replaced the mixed site (Bi/Cs) by a single atom Na (52e⁻) which represents an average of Bi^{+3} (58 e⁻) and Na^+ (26 e⁻). Distance constraints ($\text{Bi-Na} < 3.3 \text{ \AA}$, $\text{Na-Na} < 2.7 \text{ \AA}$ and $\text{Cs-Cs} < 2.3 \text{ \AA}$), ($\text{Bi-Cl} \leq 1.5 \text{ \AA}$) $\text{Na-Cl} \leq 1.2$ were applied to the search of cationic positions. A first structural model was tested based on the distribution of 18 Na atoms and 12 Bi atoms and Cl atoms over 4 crystallographic sites of multiplicities 12, 2, 8 and 4, leading to a R Bragg value of 20.4%. The first Rietveld refinement [17] on XRD data confirmed these five cationic positions, according to satisfactory R-factors (R Bragg = 11.1%, R_wp = 19.0% and R_{exp} = 2.9%). The visualisation of the structure from CIF with help of DIAMOND software programme. The particle size is 70.112 nm from FWHM and show the nano materials and can used in super conductivity. The structure of cited metal chloride is given Perovskite type structure shown in figure 4. The crystallographic data obtained after refinement shown in table 1. The bonding between atoms in octahedral cubic structure shown in table 3. The cited metal

chloride has given cubical structure and 3 dimension structure shown in figure 3. In figure 4 shown atomic position of metal chloride contained mixed valence as perovskite type structure.

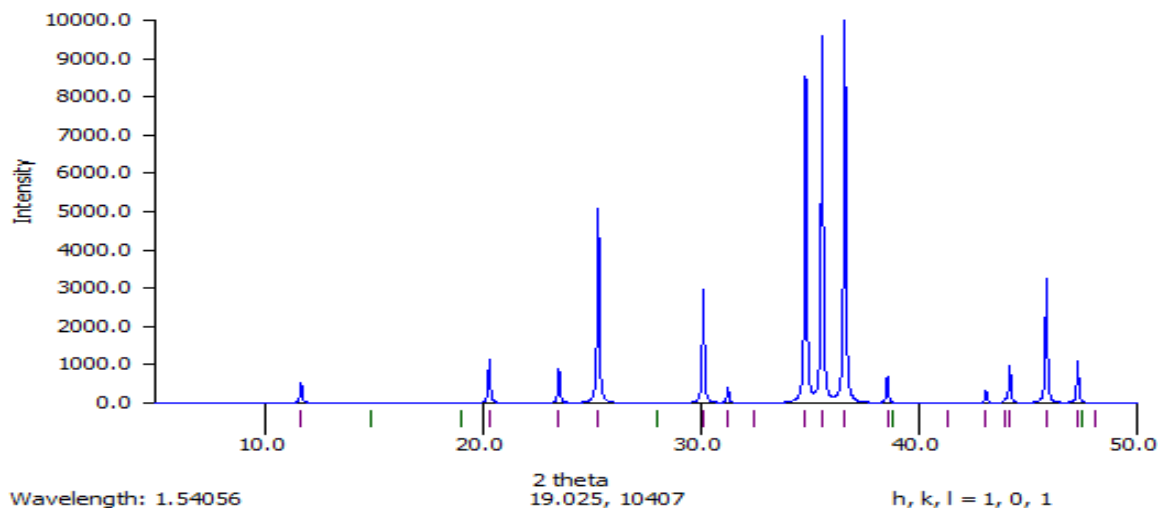


Figure 1. Powder XRD spectra of $\text{Na}_{24}\text{Bi}_4\text{Cs}_8\text{Cl}_{26}$

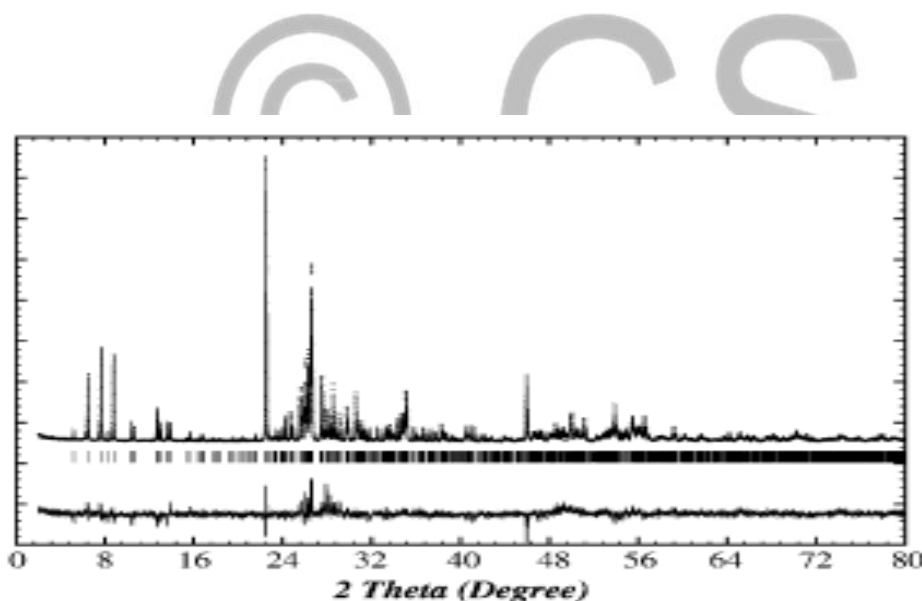


Figure 2. Graphical representation of the result from Rietveld refinement with X-ray powder data. Vertical bars indicate positions of the Bragg reflections for $\text{Na}_{24}\text{Bi}_4\text{Cs}_8\text{Cl}_{26}$ dots mark the observed intensities and the solid line gives the calculated intensity curve. The deviations between the observed and the calculated intensities from the refined model are shown by the difference plot in the lower part of the diagram and figure 5 reflected as face centre cubical structure(FCC).

Table1.Crystallgraphic data

Formula sum	Bi ₄ Cl ₂₆ Na ₂₄ Cs ₈
Formula weight	8260 g/mol
Crystal system	cubic
Space-group	F m -3 m (225)
Cell parameters	a=10.839(1) Å
Cell ratio	a/b=1.0000 b/c=1.0000 c/a=1.0000
Cell volume	1273.41(35) Å ³
Z	2
Calc. density	15.4 g/cm ³
Meas. density	15.312g/cm ³
Pearson code	cF300
Formula type	NO2P6Q66
Wyckoff sequence	e11cb6a
Index	0≤h≤-2, 1≤l≤3, 0≤l≤2

Table 2. Fraction Atomic parameters

Atom	Ox.	Wyck.	Site	S.O.F.	x/a	y/b	z/c	U [Å ²]
Bi1	+3	4a	m-3m		0	0	0	
Cl1	-1	24e	4m.m		0.246(2)	0	0	
Na1	+1	4b	m-3m		1/2	0	0	
Cl1	-1	24e	4m.m		0	0	-0.246(2)	
Cl1	-1	24e	4m.m		0	0.246(2)	0	
Cl1	-1	24e	4m.m		0	0	0.246(2)	
Cl1	-1	24e	4m.m		0	-0.246(2)	0	
Cl1	-1	24e	4m.m		-0.246(2)	0	0	
Cl1	-1	24e	4m.m		0.754(2)	0	0	
Cl1	-1	24e	4m.m		1/2	0	0.254(2)	
Cl1	-1	24e	4m.m		1/2	0	-0.254(2)	
Cl1	-1	24e	4m.m		1/2	-0.254(2)	0	
Cl1	-1	24e	4m.m		1/2	0.254(2)	0	
Na1	+1	4b	m-3m		0	0	-1/2	
Na1	+1	4b	m-3m		0	0	1/2	
Na1	+1	4b	m-3m		0	-1/2	0	
Na1	+1	4b	m-3m		0	1/2	0	
Na1	+1	4b	m-3m		-1/2	0	0	
Cs1	+3	8c	-43m		1/4	1/4	1/4	

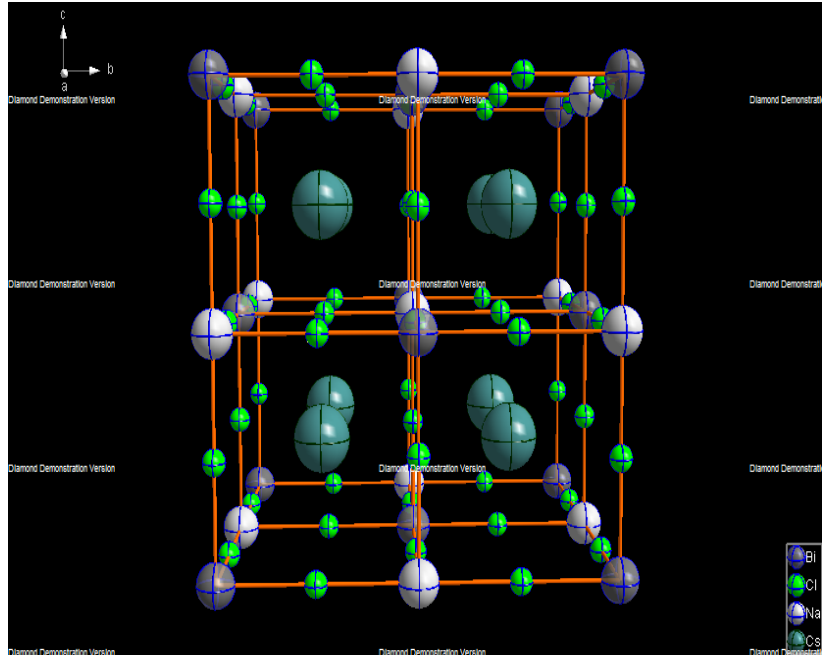


Figure3. Face centre cubical 3D structure of $\text{Na}_{24}\text{Bi}_4\text{Cs}_8\text{Cl}_{26}$

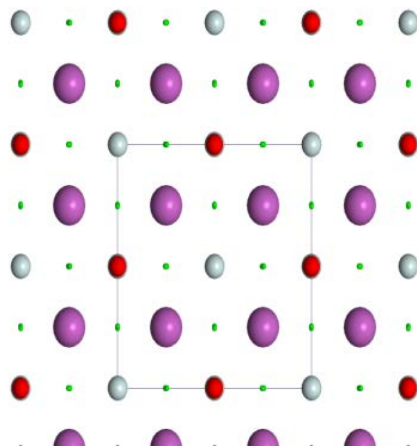


Figure4. Representation of the Perovskite -type crystal structures of $\text{Na}_{24}\text{Bi}_4\text{Cs}_8\text{Cl}_{26}$ in octahedral cubical structure.

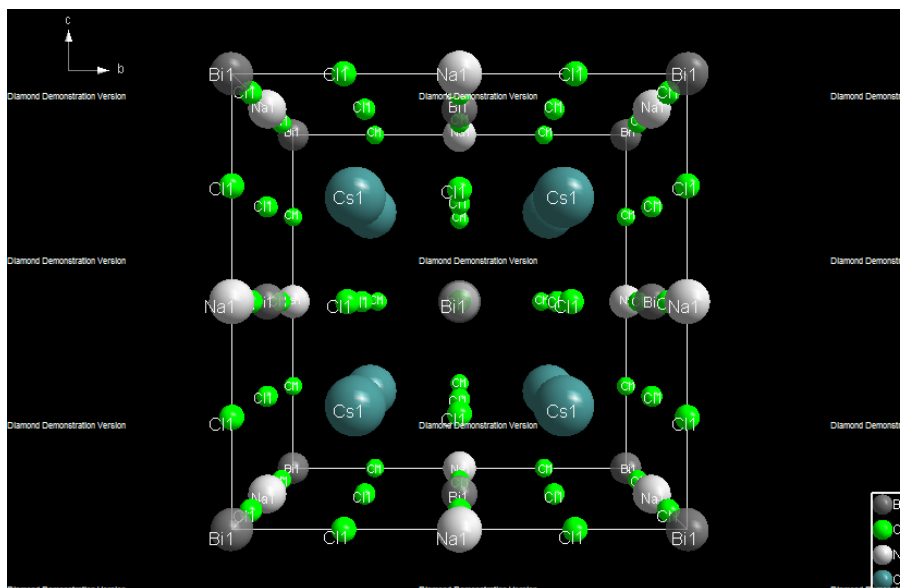
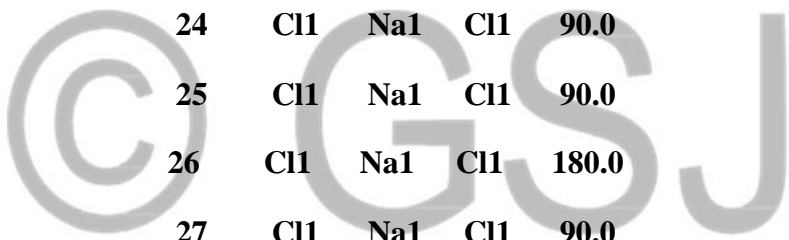


Figure 5. Face centre cubic (FCC) structure of $\text{Na}_{24}\text{Bi}_4\text{Cs}_8\text{Cl}_{26}$

Table 3. Bond angles between atoms

Number	Atom1	Atom2	Atom3	Angle($^{\circ}$)
1	Cl1	Bi1	Cl1	90.0
2	Cl1	Bi1	Cl1	90.0
3	Cl1	Bi1	Cl1	90.0
4	Cl1	Bi1	Cl1	90.0
5	Cl1	Bi1	Cl1	180.0
6	Cl1	Bi1	Cl1	90.0
7	Cl1	Bi1	Cl1	180.0
8	Cl1	Bi1	Cl1	90.0
9	Cl1	Bi1	Cl1	90.0
10	Cl1	Bi1	Cl1	90.0
11	Cl1	Bi1	Cl1	180.0
12	Cl1	Bi1	Cl1	90.0

13	Cl1	Bi1	Cl1	90.0
14	Cl1	Bi1	Cl1	90.0
15	Cl1	Bi1	Cl1	90.0
16	Bi1	Cl1	Na1	180.0
17	Cl1	Na1	Cl1	180.0
18	Cl1	Na1	Cl1	90.0
19	Cl1	Na1	Cl1	90.0
20	Cl1	Na1	Cl1	90.0
21	Cl1	Na1	Cl1	90.0
22	Cl1	Na1	Cl1	90.0
23	Cl1	Na1	Cl1	90.0
24	Cl1	Na1	Cl1	90.0
25	Cl1	Na1	Cl1	90.0
26	Cl1	Na1	Cl1	180.0
27	Cl1	Na1	Cl1	90.0
28	Cl1	Na1	Cl1	90.0
29	Cl1	Na1	Cl1	90.0
30	Cl1	Na1	Cl1	90.0
31	Cl1	Na1	Cl1	180.0
32	Bi1	Cl1	Na1	180.0
33	Bi1	Cl1	Na1	180.0
34	Bi1	Cl1	Na1	180.0
35	Bi1	Cl1	Na1	180.0
36	Bi1	Cl1	Na1	180.0



MORPHOLOGY STUDY BY SCAN ELECTRON MICROSCOPE (SEM) AND AFM

At room temperature, the morphological characterization of the $\text{Na}_{24}\text{Bi}_4\text{Cs}_8\text{Cl}_{26}$ calcined at 450°C , by AFM are shown in Figure 6. From SEM photograph of the $\text{Na}_{24}\text{Bi}_4\text{Cs}_8\text{Cl}_{26}$, the geometry of primary particles is approximately spherical due to the growth mechanism, in this case nucleation and coalescence to reach a minimum in the surface energy. The average particle size for the $\text{Na}_{24}\text{Bi}_4\text{Cs}_8\text{Cl}_{26}$ is close to 20 nm while the size of aggregates is at around 70 nm, with around 100 nanoparticles per cluster. The estimated values are for spherical clusters considered with a close packing type [18]. According to AFM technique, amplitude image (b) supplies qualitative information about the shape of the nanostructure, while the height image (c) gives significant information on sample surface topography (3D images). In the angle phase deflection images, some details of grain boundary can be observed (small image on the inferior right corner). For $\text{Na}_{24}\text{Bi}_4\text{Cs}_8\text{Cl}_{26}$ multiphase phase was identified structures in the nanometric scale, in accordance with Fig. 6. (a). In addition, a particular structure type small aggregate of size equal to 100 nm is identified being composed of a set of nanoparticles with distribution size between 15 and 30 nm, as we can see in Fig. 6. (b). The formation of small aggregates of nanoparticles is typical for material processing by chemical routes [19]. However, it is important to note that nanoparticles that forming the aggregate are weakly linked by themselves through electrostatic interactions. The average of grain size for $\text{Na}_{24}\text{Bi}_4\text{Cs}_8\text{Cl}_{26}$ is consistent with particle diameters reported elsewhere [6a]. Figure (6b) shows a set of images which project spectrum it

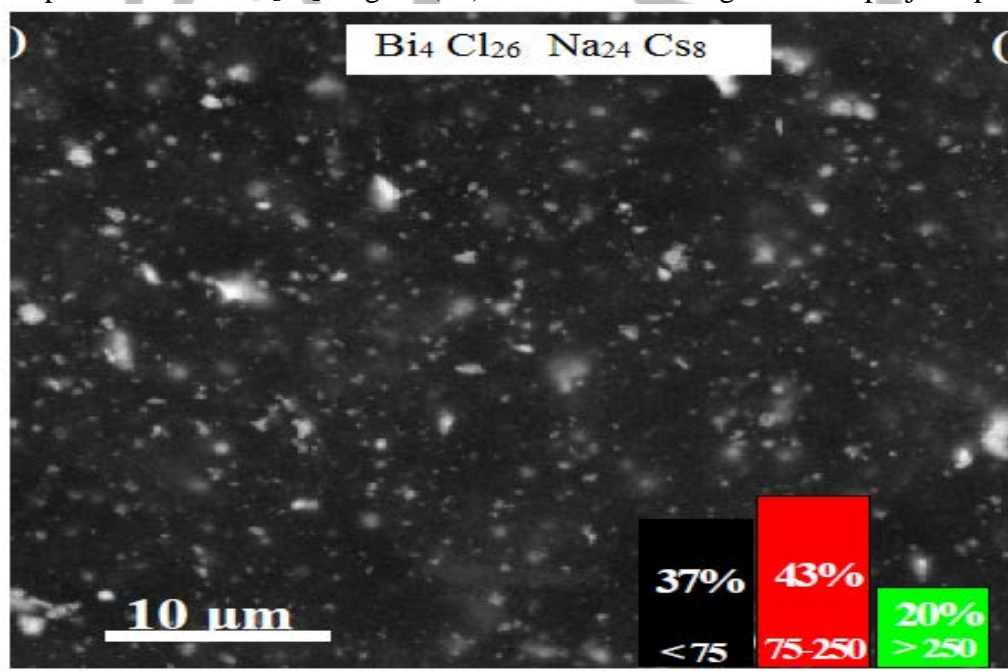


Figure 6 (a) SEM of $\text{Na}_{24}\text{Bi}_4\text{Cs}_8\text{Cl}_{26}$

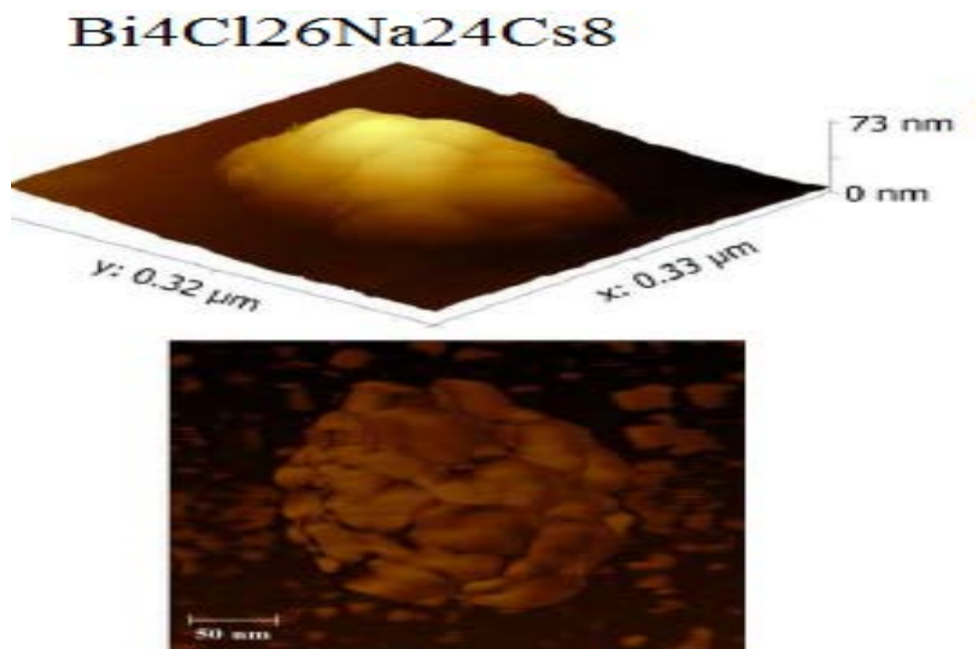


Figure 6.(b)AFM of Na₂₄Bi₄Cs₈ Cl₂₆

captured directly over the surface of the samples and their respective three-dimensional projection by AFM of vulcanized natural rubber and the ferroelectric nanocomposite formed by the addition of 10 phr of Na₂₄Bi₄Cs₈ Cl₂₆ nanopowder in a matrix of vulcanized natural rubber. Table 2 lists values of the parameter surface roughness of the ferroelectric nanocomposites as a function of the nanoparticle concentration. Both sample of vulcanized natural rubber exhibits good surface homogeneity indicating that the system and vulcanization parameters were used in a proper way. Significant differences for surface roughness were identified for the Na₂₄Bi₄Cs₈ Cl₂₆ when a low amounts of nanometric filler, as example an amount less than 5 phr, indicating that phenomena as stress-induced crystallization may be dominant [20]. It seems that differences of surface roughness observed between the ferroelectric nanocomposites can be correlated with: (i) interface filler/matrix phenomena generating changes in the folding of the polymer chains; (ii) the different thermal diffusion coefficient due to the inclusion of a ceramic phase; and (iii) directional anisotropy for the mobility of the polymer chains .Figure 6a shows SEM images for vulcanized natural rubber (a) and ferroelectric nanocomposites Na₂₄Bi₄Cs₈ Cl₂₆ 10phr. The measurements were performed directly on the fracture surface (cross section) of the samples using magnification degree of 4,000 times. According to Fig. 6(b), AFM a satisfactory volumetric homogeneity can be observed for all samples investigated indicating that set of parameters assigned to the preparation method, system and vulcanization parameters used were appropriate. The dispersion and size effect of nanometer-sized particles in the polymeric matrix, especially in rubber matrices, have been reported as having a significant impact in the mechanical properties of nanocomposites. Since nanoparticles have a strong tendency to form aggregates, because of their high surface charge and area, homogeneous dispersion of the nanoparticles in the polymer has been considered a difficult process [21].

TRANSMISSION ELECTRON MICROSCOPY (TEM)

In order to gain additional insight on crystallographic structure, microstructure, and morphology of the Na₂₄Bi₄Cs₈ Cl₂₆ samples, we performed TEM and selected area electron diffraction

(SAED) on cross-sectional samples of the material. The advantage of these methods over conventional XRD is that they provide spatially resolved structural measurements, which help to elucidate phase-purity and crystallinity of the sample at smaller length scales. A potential drawback is that the material may be damaged during sample preparation via focused-ion beam milling, and that TEM/SAED preparation and analysis can be quite time-consuming procedures. The TEM imaging shown in Figures 7 indicates that the $\text{Na}_{24}\text{Bi}_4\text{Cs}_8\text{Cl}_{26}$ layer is polycrystalline, with 80-100 nm sized columnar regions that consist of 10 nm sized crystalline particles surrounded by more disordered material. These TEM observations are consistent with the SEM results is agree with each other .Similar small-grain microstructures have been observed in other novel chloride materials in their initial stages of development. In order to analyze small areas of the sample that were inaccessible via SAED, we performed fast Fourier transforms (FFTs) of several single particles from the high-resolution[22] TEM images (represented in Figure7 .The results of this analysis indicate that crystalline areas of the $\text{Na}_{24}\text{Bi}_4\text{Cs}_8\text{Cl}_{26}$ samples are a multiphase phase, and this phase is the same across the several studies regions. Furthermore, the SAED/FFT analysis suggests that $\text{Na}_{24}\text{Bi}_4\text{Cs}_8\text{Cl}_{26}$ crystal structure has a small unit cell with low symmetry, consistent with conclusions from the prior XRD analysis.

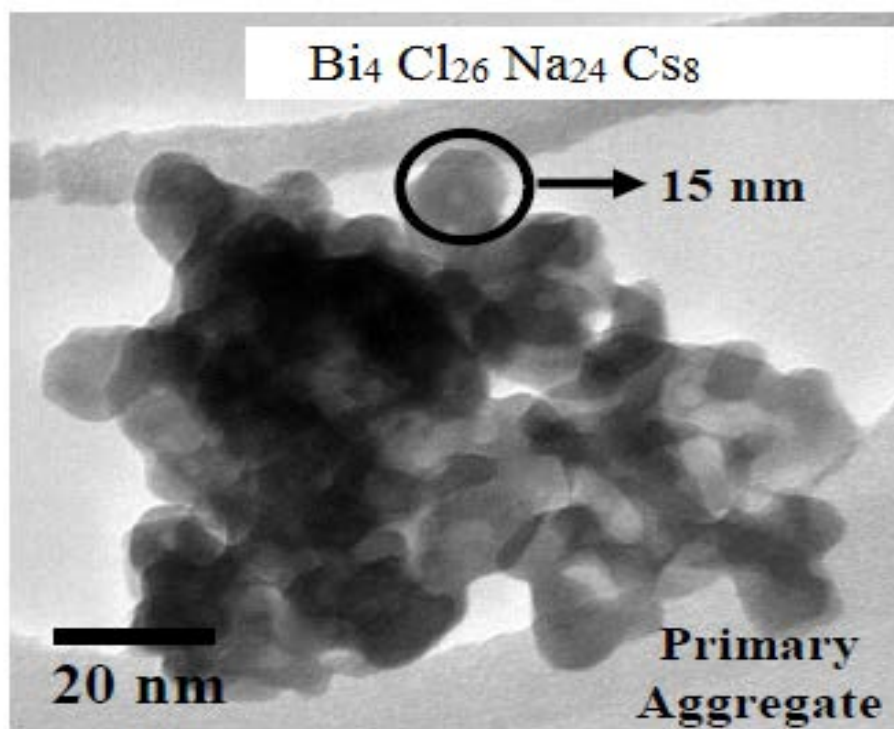


Figure 7. T E M of $\text{Na}_{24}\text{Bi}_4\text{Cs}_8\text{Cl}_{26}$

good dispersion may be achieved by surface modification of the nanoparticles under appropriate processing parameters. Secondary interactions can occur between certain functional groups attached to the nanoparticle surface and the rubber matrix, wrapping a polymer around the nanoparticle, or by using surfactants. In this sense, a good dispersion degree can be obtained using ultrafine powders with high superficial electric-charge and high surface area. Particles could be identified with nanometric dimensions (≤ 75 nm) and small aggregates (> 85 nm and ≤ 100 nm) used in the ceramic phase. Sub-micrometric particles (> 350 nm) were also found and are associated mainly with particles of the vulcanization system that are larger than the ceramic nanoparticles synthesized.

ELECTRICAL PROPERTIES

The electrical properties of the title compounds were determined by using complex impedance spectroscopy. The electrical measurements were carried out in air in the 240–360 °C temperature range after stabilization at each step of 30 °C and in the frequency range 1Hz–13MHz. The applied voltage was 0.5 V, which allows to eliminate aberrant points at low frequencies. Zview computer program [38] was used to determine the electrical parameters by using a conventional electrical circuit as follow: R//CPE-R//CPE, where CPE is a constant phase element:

$$Z_{CPE} = \frac{1}{A(j\omega)^p}$$

An additional inductance L was added to account for instrumental contributions especially at high temperature. The true capacitance was calculated from the pseudo-capacitance according to the following relationships:

$$\omega_0 = (RA)^{-1/p} = (RC)^{-1}$$

where ω_0 is the relaxation frequency, A is the pseudo-capacitance obtained from the CPE, C the true capacitance

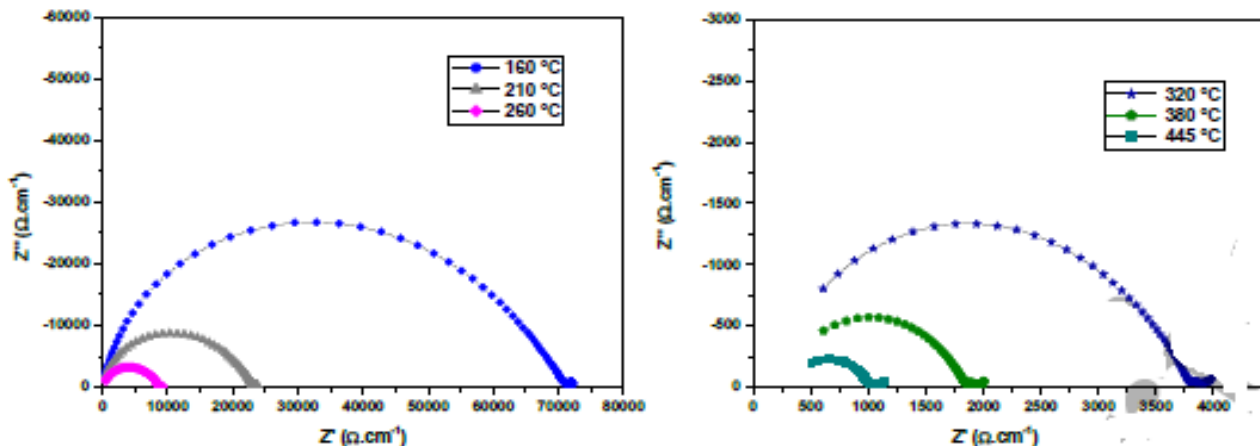


Figure 8. Normalized impedance spectra recorded on $\text{Na}_{24}\text{Bi}_4\text{Cs}_8\text{Cl}_{26}$ at 160-450 $^{\circ}\text{C}$

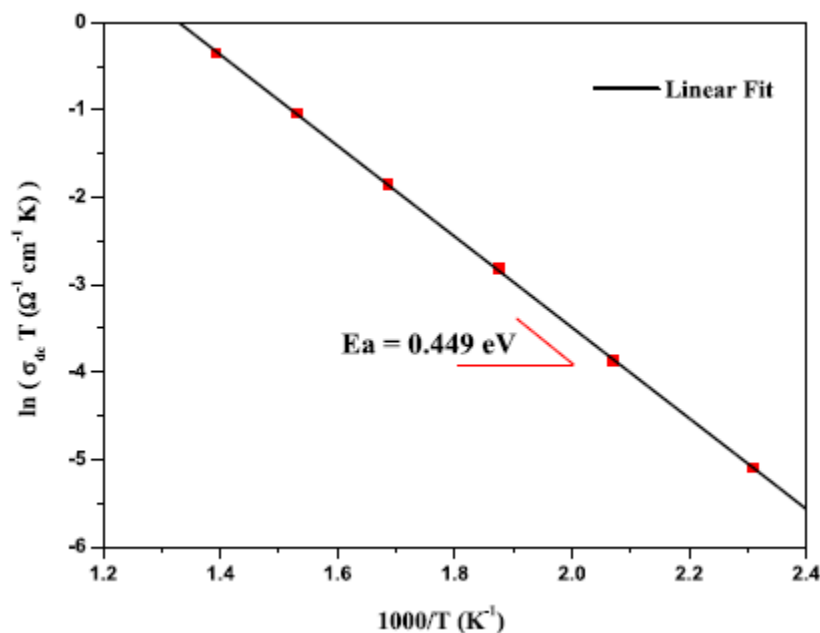


Figure 9. Arrhenius plots of conductivity of $\text{Na}_{24}\text{Bi}_4\text{Cs}_8\text{Cl}_{26}$

The electrical parameters values achieved from the equivalent circuit in the temperature range 160-445 $^{\circ}\text{C}$.. Where, the resistivity $\rho=R/k$ is extracted from the refinement of each contribution which the geometric factor of the cylindrical pellet $g(\text{cm}^{-1}) = e/S$ (e = thickness; S = surface)
 The conductivity increases from $0.14 \cdot 10^{-4} \text{ Scm}^{-1}$ at 160 $^{\circ}\text{C}$ to $9.78 \cdot 10^{-4} \text{ Scm}^{-1}$ at 445 $^{\circ}\text{C}$. Although, the absolute conductivity value of the Al/Li-substituted title material at 320 $^{\circ}\text{C}$ ($\sigma=2.64 \cdot 10^{-4} \text{ Scm}^{-1}$) is increase the increasing temperature. It should highly effective chloride batteries. The Arrhenius plot of the electrical conductivity, $\log(\sigma T (\text{S.Kcm}^{-1}))$ as a function of $1000/T (\text{K}^{-1})$, in the temperature interval 160-445 $^{\circ}\text{C}$ is illustrated in Figure 9. As a single linear plot and following the Arrhenius law, the activation energy of the $\text{Na}_{24}\text{Bi}_4\text{Cs}_8\text{Cl}_{26}$ compound determined by linear fit is 0.549 eV. Compared to previous works [21], the activation energy of the studied material is low .

CONCLUSIONS

In summary, it may be stated that at the room temperature crystal structures of three $n = 4$ Perovskite type structure of metal chloride contained mixed valence has been synthesized and refined from high resolution X-ray diffraction data by ab initio methods for structure determination and study the crystal chemistry step-by-step. The pattern decomposition and peak extraction methods have been used for the first time to derive starting models for $\text{Na}_{24}\text{Bi}_4\text{Cs}_8$

Cl_{26} . A model has been proposed for this high temperature phase. It is also confirmed that the ferroelectric to paraelectric phase transition in $\text{Na}_{24}\text{Bi}_4\text{Cs}_8\text{Cl}_{26}$ is not accompanied by a structural phase transition. The zigzag arrangement of the distorted Na^+ ions octahedral and CsCl is octahedral as observed in the $n = 2$ series of Perovskite phases are found in these structures as well. A rational explanation for the distribution of the $\text{Bi}/\text{Na}/\text{Cs}$ cations in the A sites as well as the $\text{Bi}^{+3}/\text{Na}^+$ sites is provided based on the VBS calculations. $\text{Na}_{24}\text{Bi}_4\text{Cs}_8\text{Cl}_{26}$ shows a structural transition to the prototype cubical octahedral structure in the space group $Fm\bar{3}m$ at 293K. A model has been proposed for this high temperature phase. It is also confirmed that the ferroelectric to paraelectric phase transition $\text{Na}_{24}\text{Bi}_4\text{Cs}_8\text{Cl}_{26}$ by a structural phase transition. It can be used in Na-batteries. The morphology are study by SEM, TEM and AFM. The cited compound is represent good conductor on increasing the temperature. Overall, our study suggests that tuning of the $\text{Na}_{24}\text{Bi}_4\text{Cs}_8\text{Cl}_{26}$ crystal structure geometry by doping can further improve Na ionic conductivity and thus rate capability of $\text{Na}_{24}\text{Bi}_4\text{Cs}_8\text{Cl}_{26}$ based cathodes.

REFERENCES

- [1] Zhengyang Zhou, Lukáš Palatinus, and Junliang Sun, Structure determination of modulated structures by powder X-ray diffraction and electron Diffraction Inorganic Chemistry Frontiers Doi: 10.1039/C6qi00219f
- [2] Vu, T.D.; Vu, T.D.; Barre, M.; Adil, Karim; Jouanneaux, A.; Suard, E.; Goutenoire, F. Investigation of the $\text{La}_2\text{O}_3\text{-Nb}_2\text{O}_5\text{-WO}_3$ ternary phase diagram: Isolation and crystal structure determination of the original $\text{La}_3\text{NbWO}_{10}$ material 2015 Journal of Solid State Chemistry, <http://dx.doi.org/10.1016/j.jssc.2015.05.022>
- [3]. D. Errandonea, J. Pellicer-Porres, F. Manjón, A. Segura, C. Ferrer-Roca, R. Kumar, O. Tschauner, P. Rodríguez-Hernández, J. López-Solano, S. Radescu, et al., High-pressure structural study of the scheelite tungstates CaWO_4 and SrWO_4 , Physical Review B: Condensed Matter 72 (17) (2005) 174106.
- [4]. P. Lacorre, F. Goutenoire, O. Bohnke, Designing fast oxide-ion conductors based on $\text{La}_2\text{Mo}_2\text{O}_9$, Nature 404 (2000) 856–858.
- [5] L. Malavasi, C. A. J. Fisher, M. S. Islam, Oxide-ion and proton conducting electrolyte materials for clean energy applications: structural and mechanistic features, Chemical Society Reviews ,39 (11) (2010) 4370.
- [6] Riadh Marzouki, Youssef Ben Smida, Manel Sonni, Maxim Avdeev, Mohamed Faouzi Synthesis, structure, electrical properties and Na^+ -migration pathways of $\text{Na}_2\text{CoP}_{1.5}\text{As}_{0.5}\text{O}_7$, Journal of Solid State Chemistry <https://doi.org/10.1016/j.jssc.2019.121058>
- [7]. G. Kresse, D. Joubert, From ultrasoft pseudopotentials to the projector augmented wave method, Phys. Rev. B 59 (1999) 1758–1775, <https://doi.org/10.1103/PhysRevB.59.1758>
- [8] A.P. Zhukhlistov, M.S. Nickolsky, B.B. Zvyagin, A.S. Avilov, A.K. Kulygin, S. Nicolopoulos, R. Ochs, Z. Kristallographie 219 (2004) 224.
- [9] Cabeza, A.; Losilla, E. R.; Marero-Lopez, D. Effect of Preparation Conditions on the Polymorphism and Transport Properties of $\text{La}_{6-x}\text{MoO}_{12-\delta}$ ($0 \leq x \leq 0.8$). Chem. Mater. 2017, 29, 6966–6975.
- [10] D.O. Charkin, Modular approach as applied to the description, prediction, and

Dubois, F.; Goutenoire, F.; Lalignant, Y.; Suard, E.; Lacorre, P. Ab-Initio Determination of La₂Mo₄O₁₅ Crystal Structure from X-rays and Neutron Powder Diffraction. *J. Solid State Chem.* 2001, 159, 228–233.

[11] Florian, P.; Massiot, D.; Suard, E.; Goutenoire, F. La₁₀W₂O₂₁: An Anion-Deficient Fluorite-Related Superstructure with Oxide Ion Conduction. *Inorg. Chem.* 2014, 53, 147–159. <https://doi.org/10.1007/s10870-019-00788-3>

[12] J. You, L. Xin, X. Yu, X. Zhou and Y. Liu, Synthesis of homogenous CaMoO₄ microspheres with nanopits for high-capacity anode material in Li-ion battery, *Appl. Phys. A: Mater. Sci. Process.*, 2018, 124, 271–280

[13] Lopez-Vergara, A.; Porras-Vazquez, J. M.; Infantes-Molina, A.; Canales-Vazquez, J.; mah Jebli · Abdessalem Badri · Mongi Ben Amar *Journal of Chemical Crystallography*

[14] N. Tancret, S. Obbade, N. Bettahar, and F. Abrahams *Journal of Solid State Chemistry* 124, 309–318 (1996)

[15] Parashuram Mishra, Synthesis, crystal structure determination and ionic properties of novel Bi_{1-x}Ca_{0.5x}Mg_{0.5x}O_{2.5} via X-ray powder diffraction data *Crystal Growth*. 2011, 32 (2011) 2041–2044

[16] Philipp Bertocco · Christoph Bolli · Bruno A. Correia Bicho · Carsten Jenne · Marc C. Nierstenhöfer *Journal of Chemical Crystallography* [https://doi.org/10.1007/s10870-019-00773-](https://doi.org/10.1007/s10870-019-00773-3)

[17] T. Dan Vu,† Firas Krichen,† Maud Barre,† Sandrine Coste,† Alain Jouanneaux,† Emmanuelle Suard,§ Andrew Fitch,|| and François Goutenoire targeted synthesis of bismuth oxohalides with layered structures, *Russ. J. Inorg. Chem. Suppl.* 53 (2008) 1977–1996, <https://doi.org/10.1134/S0036023608130019>.

[18] Thomas E. Weirich, Joaquim Portillo, Gerhard Cox, Hartmut Hibst, Stavros Nicolopoulos, *Ultramicroscopy* 106 (2006) 164–175

[19] Y. Liang, X. Han, Z. Yi, W. Tang, L. Zhou, J. Sun, S. Yang and Y. Zhou, Synthesis, characterization and lithium intercalation properties of rod-like CaMoO₄ nanocrystals, *J. Solid State Electrochem.*, 2007, 11, 1127–1131.

[20] Parashuram Mishra, AB Initio Structure Determination of Bi_{0.5}Mn_{0.125}Mo_{0.5}O_{0.67}U_{0.32} Mixed Valency From Quaternary of BiO₂-VO₂-UO₂-MnO-MoO₃, *International Refereed Journal of Engineering and Science (IRJES)*, Volume 9, Issue 3 (March 2020), PP. 18–24

[21] Bimal K. Kanth and Parashuram Mishra, Synthesis and structure determination of novel mixed valence Pb_{0.5}U_{0.25}Zr_{1.25}O_{4.5} by powder xrd obtained from PbCO₃-U₂(CO₃)₂-Zr₂(CO₃)₂ ternary mixed valence oxides, *International Journal For Research In Applied And Natural Science*, Volume-6 | Issue-7 | July, 2020

[22] Christopher M. Caskey, Aaron Holder, Sarah Shulda, Steven T. Christensen, David Diercks, Craig P. Schwartz, David Biagioni, Dennis Nordlund, Alon Kukliansky, Amir Natan, David Prendergast, Bernardo Orvananos, Wenhao Sun, Xiuwen Zhang, Gerbrand Ceder, David S. Ginley, William Tumas, John D. Perkins, Vladan Stevanovic, Svitlana Pylypenko, Stephan Lany, Ryan M. Richards, and Andriy Zakutayev, Synthesis of a mixed-valent tin nitride and considerations of its possible crystal structures, *The Journal of Chemical Physics* 144, 144201 (2016); doi: 10.1063/1.4945561